The activity of a novel mithramycin analogue is related to its binding to DNA, cellular accumulation, and inhibition of Sp1-driven gene transcription

Azahara Fernández-Guizán[a], Sylvia Mansilla[b], Francisca Barceló[c], Carolina Vizcaíno[b], Luz-Elena Núñez[d], Francisco Morís[d], Segundo González[a] and **José Portugal[b]***

[a] *Departamento de Biología Funcional, Facultad de Medicina, Universidad de Oviedo, E-33006 Oviedo, Spain.*

[b] *Instituto de Biología Molecular de Barcelona, CSIC, Parc Cientíific de Barcelona, E-08028 Barcelona, Spain.*

[c] *Departament de Biologia Fundamental i Ciencies de la Salut, Universitat de les Illes Balears, E-07122 Palma de Mallorca, Spain.*

[d] *EntreChem SL, Edificio Científico Tecnológico, Campus El Cristo, E-33006 Oviedo, Spain.*

*To whom correspondence should be addressed:
Dr. José Portugal
Instituto de Biologia Molecular de Barcelona, CSIC
Parc Cientific de Barcelona
Baldiri Reixac, 10
E-08028 Barcelona, Spain
Tel: +34-93-403 4959
FAX: +34-93-403 4979
E-mail: jpmbmc@ibmb.csic.es

Abbreviations: DIG-MSK, demycarosyl-3D-β-D-digitoxosyl-mithramycin SK, MSK, mithramycin SK; MTA, mithramycin A; Sp1, specificity protein 1; Sp3, specificity protein 3; TSA, trichostatin A; ULBP1, UL16-binding protein 1.

ABSTRACT

DIG-MSK (demycarosyl-3D-β-D-digitoxosyl-mithramycin SK) is a recently isolated compound of the mithramycin family of antitumor antibiotics, which includes mithramycin A (MTA) and mithramycin SK (MSK). Here, we present evidence that the binding of DIG-MSK to DNA shares the general features of other mithramycins such as the preference for C/G-rich tracts, but there are some differences in the strength of binding and the DNA sequence preferentially recognized by DIG-MSK. We aimed at gaining further insights into the DIG-MSK mechanism of action by direct comparison with the effects of the parental MTA. Similar to MTA, MSK and DIG-MSK accumulated rapidly in A2780, IGROV1 and OVCAR3 human ovarian cancer cell lines, and DIG-MSK was a potent inhibitor of both basal and induced expression of an Sp1-driven luciferase vector. This inhibitory activity was confirmed for the endogenous *Sp1* gene and a set of Sp-responsive genes, and compared to that of MTA and MSK. Furthermore, DIG-MSK was stronger than MTA as inhibitor of Sp3-driven transcription and endogenous *Sp3* gene expression. Differences in the effects of MTA, MSK and DIG-MSK on gene expression may have a large influence on their biological activities.

Keywords: Cell Uptake; DNA-binding; Mithramycin; Ovarian cancer; Transcription

1. Introduction

Mithramycin A (MTA) is an aureolic acid-type polyketide antibiotic produced by various species of *Streptomyces* [1], which has been used in the treatment of Paget's disease and advanced testicular carcinoma [2]. However, it showed numerous toxic side effects, including severe hepatotoxicity [3], which have limited its clinical use. The activity of MTA has been associated with its ability to bind to G/C-rich DNA regions via the minor groove [4-7]. It inhibits transcription both *in vivo* and *in vitro* by interfering with protein-DNA interactions [8, 9].

The genetic organization of the MTA biosynthesis gene cluster has been studied in detail, and the MTA biosynthetic pathway has been used to produce new compounds with enhanced biological characteristics [1, 4, 10-13]. Given the toxicity of MTA, the availability of analogues showing both lower toxicity and higher biological activity opens new possibilities for therapeutic applications [13, 14]. Recently, two new analogues named mithramycin SK (MSK) and DIG-MSK (demycarosyl-3D-β-D-digitoxosyl-mithramycin SK; EC-8042) (Fig. 1) have been obtained. MSK and DIG-MSK show similar *in vivo* and *in vitro* antitumor activities, but DIG-MSK is less toxic than MSK and, at least, one order of magnitude less toxic than MTA [13]. In mice, the single maximum tolerated dose of DIG-MSK is the highest among the mithramycin

analogues [13]. Furthermore, the *in vivo* evaluation of DIG-MSK antitumor activity through hollow fiber assays using 12 tumor cell lines and cancer xenograft models indicates that this compound could be a promising antitumor drug against colon, breast, ovarian, melanoma, non-small-cell lung and central nervous system cancers [13].

We have reported that several mithramycin analogues show differences in both the magnitude of their binding to DNA and the exact composition of their C/G-rich preferred binding sites. These differences might depend on the composition of their respective side chains attached at C-3 [15, 16].

Here, we compare the effects of MTA and the structurally related analogues DIG-MSK and MSK on DNA binding and cellular and nuclear accumulation in A2780, IGROV1 and OVCAR3 human ovarian cancer cell lines. MSK has profound effects on the growth and survival of those ovarian cancer cells [17], including A2780 xenografts [18], as well as on other cancer cells [19].

Several transcription factors that recognize C/G-rich tracts in promoters have been identified as potential targets for MSK and DIG-MSK, thus providing further evidence on the "transcription factor-based" action of mithramycin analogues [14, 17, 20]. The levels of Sp1 transcription factor are frequently altered in numerous human cancers [21], and the expression of Sp1 is enhanced in ovarian cancer [18]. Because MSK is a potent inhibitor of Sp1-dependent transcription both *in vitro* and in tumor xenografts [18], we explore the effects of structurally related DIG-MSK on Sp1-mediated transcription. We aimed at gaining further insights into the DIG-MSK mechanism of action by direct comparison with the effects of the parental MTA, a compound that is routinely used in different experimental systems to assess the role of the Sp1 transcription factor in gene expression, and the function of this transcription factor in cancer (see, [22-24], and references therein) as well as to abrogate *Sp1* expression *in vivo* [9]. Furthermore, we examine the effect of these mithramycins on Sp3, another member of the Sp-family of transcription factors which also binds with similar affinity to C/G-rich sequences [25]. To this end, the effect of MTA and DIG-MSK on *ULBP1* promoter activity and gene expression was also analyzed. ULBP1 is a ligand of the NKG2D receptor expressed by NK and T cells, which is involved in the immune surveillance of cancer [26, 27], and it is a predictor of poor prognosis in ovarian cancer [28]. The effects of mithramycin analogues on the *ULBP1* promoter activity are of interest because this is one of the few genes in which Sp3, but not Sp1, is a key gene regulator, increasing more than 500-fold the *ULBP1* promoter activity [26, 27]. We observed that the effect of the novel DIG-MSK on transcription depends on the cell line examined and, in general, it is equivalent, or even stronger, than the parental MTA.

2. Materials and methods

2.1. Mithramycins

Mithramycin A (MTA), mithramycin SK (MSK) and demycarosyl-3D-β-D-digitoxosyl-mithramycin SK (DIG-MSK; EC-8042) were isolated and purified from the producing organisms as described previously [4, 13], and their purity (≥ 97%) was checked by HPLC. Stock solutions of the different compounds were prepared at either 10 mM in DMSO or 500 mM in 50 mM NaCl, 20 mM Hepes (pH 7.5), kept at -20°C, and diluted to the desired concentration before the experiments, using the same buffer or tissue culture medium. When required for the different experiments, $MgCl_2$ was added to the same buffer at various concentrations in the 1 to 3 mM range.

2.2. Fluorescence spectroscopy

Fluorescence spectroscopy experiments were carried out in a Cary Eclipse fluorescence spectrophotometer (Varian Inc.) using 1-cm pathlength, as described previously [16] with minor modifications. In brief, DNA binding was measured by fluorescence titration (λ_{ex}: 410 nm, λ_{em}: 548 nm) of 22 μM solutions of DIG-MSK dissolved in 50 mM NaCl, 20 mM Hepes (pH 7.5) containing either 1, 1.5 or 3 mM $MgCl_2$ and incubated for 1 h at 25 ºC or 37 ºC to ensure the Mg^{2+}-mediated dimerization of the compounds. Small aliquots of sonicated calf thymus DNA (Sigma) in the same buffer were added to the drug solutions and the fluorescence spectra obtained after 3 min equilibrium at both 25 ºC and 37 ºC.

2.3. Thermal denaturation studies

Ultraviolet DNA melting curves were determined using a Jasco V-650 spectrophotometer equipped with an ETC-505T (Jasco) temperature controller. Samples contained 20 μM (in bp) sonicated calf thymus DNA (Sigma) and either MTA, MSK or DIG-MSK to obtain drug/DNA molar ratios of 0.25 (enough to saturate the potential drug-binding sites [16]) in 50 mM NaCl, 20 mM Hepes (pH 7.5) containing 1 mM $MgCl_2$. The samples were equilibrated at 25 °C for 30 min and then heated at a rate of 1 °C min^{-1}, while continuously monitoring the absorbance at 260 nm. The Spectra Manager software (Jasco) was used to analyze the data and to calculate the DNA melting temperature (Tm).

2.4. Restriction enzyme cleavage assays

The effects of the different mithramycin analogues on the first-order rate constant at the individual restriction enzyme sites were determined as described elsewhere [15]. In brief, plasmid pBR322 was linearized by cleavage with *BamHI* (Fermentas). *Bsp68I* (*NruI*) and *Eco52I* (*EagI*) from Fermentas were used for restriction enzyme assays using the buffers supplied by the vendor. These two enzymes cleave the pBR322 plasmid at unique sites. DNA

cleavage reactions containing 40 μM (in bp) DNA and 8 μM MTA, MSK or DIG-MSK (corresponding to a 0.20 drug/DNA (bp) molar ratio) were pre-incubated at 25 °C for 20 min, and the cleavage reactions initiated at 37 °C by the addition of the appropriate enzyme. Time-course digestion products were resolved by electrophoresis on 1.2% agarose gels. After running, the gels were stained with ethidium bromide, documented using a GeneGenius BioImaging system and quantified. Linear-least-squares fit of the logarithm of the relative amount of uncut DNA *versus* time renders the first-order rate constant for cleavage at each restriction site [29].

2.5. Cell culture

A2780, OVCAR3 and IGROV1 human ovarian carcinoma cell lines were grown in RPMI 1640 medium (Invitrogen) supplemented with 10% heat-inactivated fetal calf serum (Invitrogen), 2 mM L-glutamine, 1 mM pyruvate, and 200 mg/ml gentamicin, at 37 °C in a humidified atmosphere with 5% CO_2.

2.6. Cellular accumulation of mithramycin analogues

Ovarian cancer cells ($1x10^4$ cells) were incubated in RPMI 1640 medium with either DMSO or 100 mM of each mithramycin analogue. After 2 and 4 hours incubation, cells were repeatedly washed with ice-cold phosphate-buffered saline (PBS), harvested and immediately analyzed using a BD FACSCanto flow cytometer. Isolation of intact nuclei was carried out as described elsewhere [17]. Nuclei yield and integrity were confirmed by Trypan blue staining and microscopic examination.

2.7. Transient transfections and luciferase reporter assays

A2780, OVCAR 3 and IGROV1 cells were transfected with 300 ng of the TransLucent Sp1 reporter (Sp1-Luc) from Panomics or the ULBP1 reporter [26] and 12 ng of pRL-null vector (Promega) as internal control, by using Lipofectamine 2000 (Invitrogen) following the manufacturer's recommendations. Briefly, $5x10^3$ cells were transfected in 12-well plates, and 200 nM MTA or DIG-MSK —a concentration that would reduce cell population by 90% after 72-h treatments, according to Trypan blue staining— were assayed as inhibitors of Sp-driven transcription, which was examines after 24-h, when most of the cells remained viable. For experiments carried out in the presence of the deacetylase inhibitor TSA (trichostatin A, Sigma), this compound was prepared in DMSO and added to cells at 500 nM, followed by addition of 200 nM MTA or DIG-MSK. Cultures containing the same amount of DMSO were used as controls for the different experiments. Each mithramycin analogue was added 4 hours after DNA transfections, either in the absence or in presence of TSA, and the expression levels analyzed after 24 h. To assess the effect of the mithramycins on cells overexpressing either Sp1 or Sp3, the different cell lines were co-transfected with 400 ng of either pN3-Sp1FL or pN3-Sp3FL

expression plasmids and pN3 empty vector (used to normalize for the transfection efficiency) — all of them kindly supplied by Dr. G. Suske (Philipps-Universität Marburg, GE)—, together with 100 ng of the Sp1-Luc reporter (Panomics) by using the protocol described above (this reporter vector contains a C/G-rich box that can be also recognized by other members of the Sp-family of transcription factors). Each mithramycin analogue (200 nM final concentration) was added 4 hours after DNA transfections. Luciferase activity was assayed using the Dual Luciferase Reporter System (Promega) and a Turner BioSystems TD20/20 luminometer.

2.8. Quantitative real-time RT-PCR assays

Total RNA was isolated from control cells (those to which no drug was added) and from cells treated with MTA, MSK or DIG-MSK for either 8 h or 24 h, depending on the experiment (see Section 3). Total RNA was extracted from cells using the High Pure RNA Isolating kit (Roche Diagnostics) and cDNA was obtained using the High Capacity cDNA Reverse Transcription Kit (Invitrogen) according to the manufacture's protocols. Quantitative real-time RT-PCR (qRT-PCR) experiments were performed in either a 7900HT Real-Time System (Applied Biosystems), using the SYBRGreen PCR Master Mix (Applied Biosystems), or in a Roche LightCycler 480, using the SYBR-Green PCR Master Mix (Roche Diagnostics). The primers used for qRT-PCR are shown in Table 1. PCR conditions included an initial denaturation step at 95 °C for 3 min, followed by 40 cycles at 95 °C for 20 s and an annealing step at 60 °C for 30 s, and an elongation step at 72 °C for 30 s. A final dissociation curve was generated to verify that a single product was amplified. Reactions in the absence of template and in the absence of enzyme were also included as negative controls. Relative expression values of the different genes were calculated from the threshold cycle (C_t) following the $\Delta\Delta C_t$ method using *GAPDH* as an internal housekeeping control for gene expression normalization.

2.9. Statistical analysis

Statistical analysis was performed using SPSS v.20 (IBM Corp.) software. Results represent the mean ± SD, or mean ± SEM, values of three to six experiments. Two sample group differences were evaluated using the Student's t-test. Depending on the data characteristics and the number of independent experiments performed, multiple group comparison were assessed by either Kruskal–Wallis one-way analysis of variance and further pairwise Mann-Whitney U test analysis, or by one-way ANOVA with Tukey's post hoc test.

3. Results

3.1. The binding of DIG-MSK to DNA shows some differences compared to that of other mithramycins

As a first approach, we explored the binding of MTA, MSK and DIG-MSK to DNA by monitoring changes in DNA melting temperature (Tm) calculated from absorbance (at 260 nm) *versus* temperature melting curves in the presence of mithramycin analogues (Table 2). The raise of Tm values obtained at a 0.25 drug/DNA (bp) molar ratio that corresponds to a binding stoichiometry of 4 mol of DNA (bp) per mol of drug —enough to saturate the potential G/C-rich binding sites in heterogeneous DNA [16]— indicated that all mythramycins bind to DNA and that the parental MTA binds tighter than MSK or DIG-MSK.

Fluorescence titration experiments showed that DIG-MSK solutions titrated with increased concentration of calf thymus DNA behaved rather different in experiments performed at 25 ºC (Fig. 2A) and at 37 ºC (Fig. 2B). While at 25 ºC fluorescence increased after adding higher concentrations of DNA, the same kind of experiments carried at 37 ºC showed that fluorescence was quenched. Moreover, after that an ~5-6 DNA (bp)/drug molar ratio was reached there was no significant increase/decrease in fluorescence at either temperature, and therefore it was not possible to obtain experimental values that could be used to fit accurately binding models that require the emission intensity to be linearly proportional to the concentration of the drug [16]. These results did not depend on the $MgCl_2$ concentration used (see Section 2). We have previously described the thermodynamic parameters of MSK binding to DNA based on similar fluorescence titrations, which rendered and apparent binding constant of 1.2×10^4 M^{-1} in a buffer containing 1.5 mM $MgCl_2$ [16]. In any case, from a mere qualitative point of view the superior protection of DNA melting by MSK (Table 2) would indicate that MSK binds DNA tighter than DIG-MSK.

As a quantification of DIG-MSK binding was not attained, we followed a different approach to explore whether the difference between MSK and DIG-MSK sugar moieties (Fig. 1) may result in differences in the DNA sequence that is preferentially recognized by the two analogues. To this end, we analyzed the differential inhibition of restriction enzyme cleavage by MTA, MSK and DIG-MSK on a linearized DNA plasmid (Fig. 3). MTA protected better than MSK or DIG-MSK both 5'-TCGCGA-3' (*Bsp68I*) and 5'-CGGCCG-3' (*Eco52I*) sequences from digestion (Fig. 3). Moreover, MSK was superior to DIG-MSK in abrogating *Eco52I* cleavage ($p < 0.05$*;* Fig. 3B). Roughly speaking, the higher Tm values in the presence of MSK (Table 2) as well as the superior protection of 5'-CGGCCG-3' tracts by MSK (Fig. 3) were consistent with that MSK binds to DNA tighter than DIG-MSK, and that MSK can be more prone to accept different C/G-rich sequence arrangements at the binding site. The differences observed between the binding of MSK and DIG-MSK were a consequence of the distinct sugar E in the trisaccharide chain (Fig. 1), which can entail changes in the interaction with DNA.

3.2. DIG-MSK accumulated in human ovarian tumor cell lines

Given that previous studies had revealed that mithramycins are highly active in gynecological cancer [17, 18], we sought to unveil whether the cellular and nuclear accumulation of MTA, MSK and DIG-MSK in three human ovarian carcinoma cell lines was equivalent. Figure 4 shows that every mithramycin analogue fairly accumulated after 2h, while larger 4-h incubations did not result in a significant increase in drug accumulation. The three compounds also reached the nuclei of all the cell lines within 2 h. A comparison of the uptake of MTA or MSK between 2-h and 4-h treatments showed a time-dependent nuclear accumulation in IGROV1 and OVCAR3 cells (see legend to Fig. 4). DIG-MSK accumulated in OVCAR3 nuclei with significant differences between 2-h and 4-h treatments, yet the drug levels were lower than of MTA (Fig. 4). These experiments on cellular and nuclear accumulation indicated that the behavior of the mithramycins depended on the ovarian cell line used and the incubation time.

3.3. DIG-MSK is a potent inhibitor of Sp1-driven transcription and Sp1 expression

Because several mithramycins have been characterized as potent inhibitors of Sp1-activated transcription, we examined the effects of DIG-MSK on the expression of a transfected luciferase reporter vector containing several Sp1 response elements (CG-boxes). Since MTA is routinely used as a tool to assess whether Sp1 transactivates a variety of promoters *in vivo* (cell culture), we employed it as a control to be compared to the new DIG-MSK in experiments undertaken in ovarian cancer cell lines. DIG-MSK retains the capacity of MTA to potently inhibit Sp1-driven promoter activity in A2780 and OVCAR3 cells, and it significantly inhibits ($p < 0.01$) the transcriptional activity in IGROV1 cells (Fig. 5A). To strength the evidence, the effect of mithramycins on the Sp1-mediated promoter activity was also analyzed in cells treated with trichostatin A (TSA), an inhibitor of histone deacetylases that enhances Sp1-activation levels [30]. Figure 5B shows that even in the presence of TSA, MTA and DIG-MSK markedly reduced luciferase levels.

To characterize how the alteration of Sp1 levels impinge on the effect of DIG-MSK against the expression of Sp1-driven report plasmids, the Sp1-mediated promoter activity was enhanced by the transient co-transfection of an Sp1 expression vector in the different ovarian cell lines. Sp1 over-expression enhanced about 15-fold the expression of the reporter plasmid in IGROV1 cells and about 3-fold in A2780 and OVCAR3 cells. In the presence of Sp1 expression vector, DIG-MSK showed an “anti-transcriptional effect” similar to that of the parental MTA in A2780 and OVCAR3 cells, whereas the relative inhibition was clearly higher in IGROV1 cells when compared to untreated cells (Fig. 5C).

Given that the *Sp1* gene is regulated by itself in a feedback positive manner, we next assessed the effects on the transcription of endogenous gene by treating ovarian cells with MTA and DIG-MSK, and the expression of the endogenous *Sp1* was measured by qRT-PCR. DIG-MSK produced a significant inhibition ($p < 0.01$) of the expression of *Sp1* in both A2780 and IGROV1 cells, which, nevertheless, was similar to that of MTA (Fig. 5D). Taken together, these experiments indicate that DIG-MSK is a potent inhibitor of Sp1-mediated transcription and *Sp1* gene expression in ovarian cells, a property it shares with the other mithramycin analogues.

3.4. DIG-MSK is stronger than MTA as inhibitor of Sp3 expression and Sp3-mediated transcription

Sp3 is a member of the family of Sp1-related genes that also binds to C/G-rich boxes. We examined the capacity of DIG-MSK for inhibiting Sp3-driven transcription. As a first approach, a luciferase reporter plasmid under the control of the ULBP1 promoter was used since Sp3 is a potent and specific regulator of *ULBP1* transcription, which is able to induce more than 500-fold the promoter activity of the gene [26]. MTA and DIG-MSK inhibited ULBP1 promoter activity in A2780 and IGROV1, while the inhibitory capacity of DIG-MSK was higher than of MTA in IGROV1 cells (Fig. 6A). Sp1 stimulates the activity of a variety of promoters, while Sp3 is a bifunctional transcription factor that either stimulates or represses the transcription of *ULBP1*, among other genes. Interestingly, the luciferase activity driven by the ULBP1 promoter activity was up-regulated in OVCAR3 cells by MTA and DIG-MSK (Fig. 6A). Seemingly, in this cell line Sp3 could gain access to the promoter acting as activator in the presence of the compounds, yet the three ovarian cell lines can differ in the abundance and activity of the Sp3 isoforms. To further characterize the effect of DIG-MSK on Sp3-mediated promoter activity, Sp3 was over-expressed in the ovarian cell lines by transient transfection of an Sp3-expression vector and the promoter activity was analyzed by using a luciferase reporter vector that contains several C/G-rich response elements. DIG-MSK was stronger than MTA in inhibiting the promoter activity induced by Sp3 over-expression in the three ovarian cell lines (Fig. 6B).

The effect of MTA and DIG-MSK on the expression of the endogenous *Sp3* and *UBLP1* genes was also measured by qRT-PCR. With regard to *Sp3* gene inhibition, MTA and DIG-MSK down-regulated its expression in OVCAR3 and IGROV1 cells, while no significant changes were observed in A2780 cells (Fig. 6C). DIG-MSK was significantly stronger than MTA ($p < 0.01$) in inhibiting the endogenous *Sp3* gene in OVCAR3 and IGROV1 cells. DIG-MSK significantly inhibited the *UBLP1* gene ($p < 0.01$) in the three ovarian cell lines (Fig. 6D), while MTA enhanced its expression in IGROV1 cells ($p < 0.05$). Moreover, DIG-MSK had a higher inhibiting effect on *ULBP1* expression in IGROV1 and OVCAR3 cells. Taken together, these

results suggested that DIG-MSK did not only inhibit Sp1-induced transcription but also altered Sp3-mediated transcription in ovarian cell lines. Although the down-regulation of the *Sp1* gene can result in a shortage of Sp1 factor, our luciferase reporter assays suggest that the final outcome in cells treated with DIG-MSK depended on the direct competition between Sp1 and DIG-MSK for consensus binding sequences in gene promoters, consistent with our previous *in vitro* EMSA (electrophoretic mobility assays) that showed that DIG-MSK displaces Sp1 from its putative binding sites [20].

3.5. The novel mithramycin analogue DIG-MSK down-regulated the expression of a variety of endogenous genes in human ovarian cancer cells

To further assess the relevance of the effects of DIG-MSK on gene expression, we studied a set of Sp1/Sp3-responsive endogenous genes and compared the changes in gene expression with those induced by MTA or MSK. The set included genes involved in the control of gene transcription (*E2F1*), cell cycle (*CCNB1*) or angiogenesis (*VEGF-C*). Figure 7 shows their relative expression in the three ovarian cell lines together with that of *Sp1*, *Sp3* and *ULBP1*. The three compounds abrogated the expression of the angiogenesis-related *VEGF-C* gene in all the ovarian cell lines. The *CCNB1* (*cyclin B1*) gene was more down-regulated by DIG-MSK than by its analogues in A2780 cells (Fig. 7A). However, DIG-MSK was not efficient in abrogating the expression of *E2F1* in A2780 cells (Fig. 7A), whereas it was rather active on the same gene in the other ovarian cancer cells (Figs. 7B and 7C). Besides, the three compounds did not down-regulate the endogenous *Sp1* gene in OVCAR3 cells (Fig. 7C). In IGROV1 and OVCAR3 cells *Sp3* expression was strongly reduced, with a superior effect of DIG-MSK (Figs. 7B and 7C). DIG-MSK was a strong inhibitor of both *Sp3* and the *ULBP1* gene expression, the latter being strongly Sp3-dependent, as described above.

4. Discussion

MSK has an improved therapeutic index compared to the parental MTA [4, 17] and it inhibits the transcription of several genes [17, 31], which is likely to occur, at least in part, by direct abrogation of the Sp1-transactivating effects on gene expression [14, 32]. Here, we show that the novel analogue DIG-MSK also binds to DNA and it alters gene expression, which may be a desirable mechanism of intervention in certain cancers [33]. Furthermore, DIG-MSK entails an improved pharmacological profile with high antitumor activity and less toxicity [13].

In a previous paper, we calculated by fluorescence titration the binding of several mithramycin analogues to DNA [16]. However, when we used the same approach to analyze the DNA binding of the new DIG-MSK we did not obtain a reliable apparent binding constant

(K_{obs}), see Section 3. DIG-MSK shows a rather peculiar behavior because its fluorescence was enhanced or quenched by DNA depending on the temperature. We are at a loss to explain why such fluorescence behavior ensued, although examples exist of DNA-binding agents which fluorescence can be enhanced or quenched upon binding [34]. In our experiments it is peculiar that this phenomenon is observed with the same molecule binding to DNA at different temperatures. From a qualitative point of view, we can infer that the binding of DIG-MSK to DNA is similar to that of other MTA analogues, thus producing changes in gene expression.

We used a promoter-luciferase reporter driven by Sp1-responsive elements to characterize whether DIG-MSK interferes with basal and induced Sp1-driven transcription (Fig. 5). The effects of DIG-MSK on gene expression are higher than of MTA in some ovarian cell lines (Figs. 5-7). Sp1 is a well-known member of a growing family of transcription factors that also includes Sp3, which display similar DNA binding characteristics, but also some different functional properties [22, 25, 35]. Together with the effect of mithramycins on Sp1, we have also analyzed the effects on Sp3-mediated transcription and *Sp3* gene expression. To differentiate the specific effects of Sp3 from Sp1 ones, we assessed the effects of DIG-MSK on the ULBP1 promoter activity. *ULBP1*, a predictor of poor prognosis in ovarian cancer patients [28], is one of the few genes in which Sp3, but not Sp1, has been reported to be a specific and strong regulator of its transcription [26]. The effect on Sp3-mediated transcription was further analyzed by over-expressing Sp3 in the ovarian cell lines. In general, DIG-MSK is equivalent or significantly stronger than the parental MTA in inhibiting Sp3-mediated transcription. DIG-MSK has a superior inhibiting effect on the expression of endogenous *Sp3* and *ULBP1* genes (Figs. 6 and 7). Because of the ubiquitous expression of Sp3, and its role in regulating a wide variety of genes, we suggest that such differences may contribute to the distinct pharmacological profile of DIG-MSK. In OVCAR3 cells, the three mithramycins had little effect on *Sp1* gene expression, regardless of their effects on other endogenous Sp1-responsive genes (Fig. 7C). This peculiarity may arise from the large polymorphism observed in the Sp1/Sp3 binding-sites in OVCAR cells, which could protect them against time-dependent silencing [36].

Given that Sp1 is an important regulator of the expression of multiple angiogenic factors [22], the down-regulation of *VEGF-C* by the new MSK and DIG-MSK (Fig. 7) might have clinical implications, as it has been suggested for the parental MTA [9]. DIG-MSK would be advantageous on account of its lower toxicity. The superior effect of DIG-MSK on the expression of *CCNB1 (cyclin B1)* in A2780 cells (Fig. 7A) is consistent with the effects of this compound on genes involved in cell cycle control in colon carcinoma cells [20]. In transfected IGROV1 cells the down-regulation of Sp1-driven luciferase expression, as well as the down-

regulation of a set of cellular genes which includes *Sp1*, *Sp3* and *ULBP1*, by DIG-MSK correlates with its superior antitumor effect on these cells [13].

All the mithramycin analogues bind to DNA significantly and they interfere with the transcription machinery. Nevertheless, the improved characteristics of MSK and DIG-MSK can be a consequence of other aspects like their selective accumulation in certain cells and tissues, (Fig. 4 and [13, 15, 17]). In fact, the lower systemic toxicity of DIG-MSK suggests a selective distribution of this analogue [13], in keeping with our results. Altogether, the novel DIG-MSK is interesting in the pursuit of improved targeting in the treatment of ovarian cancer [37].

In summary, the distinctive antitumor activities of MSK and DIG-MSK against several experimental models and the different cytotoxic effects might be attributed to the differential capacity of these molecules for traversing cell membranes, which can result in direct binding to DNA, and, in general, in making gene expression rather sensitive to the mithramycins. The improved pharmacological and toxicological profiles of novel mithramycin analogues such as MSK and DIG-MSK provide us with grounds for considering that new possibilities exist for taking advantage of the unique characteristics of these compounds for therapeutic applications.

Conflict of interest

L-EN and FM are employees of EntreChem SL. FM reports ownership of stock in EntreChem SL**.** All other authors declare they have no conflict of interests.

Acknowledgments

We thank José L. Insua for helping us in the fluorescence experiments. This work was supported by grant BFU2010-15518 from the Spanish Ministry of Science and Innovation, and the FEDER program of the European Community, and it was performed within the framework of the "Xarxa de Referencia en Biotecnologia" of the Generalitat de Catalunya. It was also supported by the Principado de Asturias Government through PCTI founds 2006-2009, 80% co-financed with the FEDER Operative Program of the Principado de Asturias 2007-2013 (project FC-11-PC-10-31) and Fondo de Investigaciones Sanitarias (Institute Carlos III) PS09/00420 and PI12/01280. A. F-G. is co-financed by the project COF-11-24 from FICYT. C.V. is recipient of a JAE-Predoc2010 fellowship (CSIC), co-financed by the European Social Fund.

REFERENCES

[1] F. Lombó, N. Menéndez, J.A. Salas, C. Méndez, The aureolic acid family of antitumor compounds: structure, mode of action, biosynthesis, and novel derivatives, Appl. Microbiol. Biotechnol., 73 (2006) 1-14.

[2] V.T.Jr. DeVita, S. Hellman, S.A. Rosenberg, Cancer: Principles & Practice of Oncology, 7th ed., Lippincott Williams & Wilkins, Philadelphia, PA, 2005.

[3] P.D. King, M.C. Perry, Hepatotoxicity of chemotherapy, Oncologist 6(2001) 162-176.

[4] L.L. Remsing, A.M. González, M. Nur-e-Alam, M.J. Fernández-Lozano, A.F. Braña, U. Rix, M.A. Oliveira, C. Méndez, J.A. Salas, J. Rohr, Mithramycin SK, A novel antitumor drug with improved therapeutic index, mithramycin SA, and demycarosyl-mithramycin SK: Three new products generated in the mithramycin producer *Streptomyces argillaceus* through combinatorial biosynthesis, J. Am. Chem. Soc., 125 (2003) 5745-5753.

[5] M. Sastry, D.J. Patel, Solution structure of the mithramycin dimer-DNA complex, Biochemistry, 32 (1993) 6588-6604.

[6] A.J. Hampshire, K.R. Fox, The effects of local DNA sequence on the interaction of ligands with their preferred binding sites, Biochimie 90 (2008) 988-998.

[7] F. Barceló, C. Scotta, M. Ortiz-Lombardía, C. Méndez, J.A. Salas, J. Portugal, Entropically-driven binding of mithramycin in the minor groove of C/G-rich DNA sequences, Nucleic Acids Res., 35 (2007) 2215-2226.

[8] D.E. Jones, Jr., D.M. Cui, D.M. Miller, Expression of β-galactosidase under the control of the human c-myc promoter in transgenic mice is inhibited by mithramycin, Oncogene 10 (1995) 2323-2330.

[9] Z. Jia, J. Zhang, D. Wei, L. Wang, P. Yuan, X. Le, Q. Li, J. Yao, K. Xie, Molecular basis of the synergistic antiangiogenic activity of bevacizumab and mithramycin A, Cancer Res., 67 (2007) 4878-4885.

[10] D. Rodríguez, L.M. Quirós, J.A. Salas, MtmMII-mediated C-methylation during biosynthesis of the antitumor drug mithramycin is essential for biological activity and DNA-drug interaction, J. Biol. Chem., 279 (2004) 8149-8158.

[11] M. Pérez, I. Baig, A.F. Braña, J.A. Salas, J. Rohr, C. Méndez, Generation of new derivatives of the antitumor antibiotic mithramycin by altering the glycosylation pattern through combinatorial biosynthesis, Chembiochem., 29 (2008) 2295-2304.

[12] B. García, J. González-Sabin, N. Menéndez, A.F. Braña, L.E. Nuñez, F. Morís, J.A. Salas, C. Méndez, The chromomycin CmmA acetyltransferase: a membrane-bound enzyme as a tool

for increasing structural diversity of the antitumour mithramycin, Microb. Biotechnol., 4 (2011) 226-238.
[13] L.E. Núñez, S.E. Nybo, J. González-Sabín, M. Pérez, N. Menéndez, A.F. Braña, M. He, F. Morís, J.A. Salas, J. Rohr, C. Méndez, A novel mithramycin analogue with high antitumor activity and less toxicity generated by combinatorial biosynthesis, J. Med. Chem., 55 (2012) 5813-5825.
[14] A. Malek, L.E. Nuñez, M. Magistri, L. Brambilla, S. Jovic, G.M. Carbone, F. Moris, C.V. Catapano, Modulation of the activity of Sp transcription factors by mithramycin analogues as a new strategy for treatment of metastatic prostate cancer, PLoS One 7(2012) e35130.
[15] S. Mansilla, I. Garcia-Ferrer, C. Méndez, J.A. Salas, J. Portugal, Differential inhibition of restriction enzyme cleavage by chromophore-modified analogues of the antitumour antibiotics mithramycin and chromomycin reveals structure–activity relationships, Biochem. Pharmacol., 79 (2010) 1418-1427.
[16] F. Barceló, M. Ortiz-Lombardía, M. Martorell, M. Oliver, C. Méndez, J.A. Salas, J. Portugal, DNA binding characteristics of mithramycin and chromomycin analogues obtained by combinatorial biosynthesis, Biochemistry 49 (2010) 10543-10552.
[17] V. Albertini, A. Jain, S. Vignati, S. Napoli, A. Rinaldi, I. Kwee, M. Nur-e-Alam, J. Bergant, F. Bertoni, G.M. Carbone, J. Rohr, C.V. Catapano, Novel GC-rich DNA-binding compound produced by a genetically engineered mutant of the mithramycin producer *Streptomyces argillaceus* exhibits improved transcriptional repressor activity: implications for cancer therapy, Nucleic Acids Res., 34 (2006) 1721-1734.
[18] S. Previdi, A. Malek, V. Albertini, C. Riva, C. Capella, M. Broggini, G.M. Carbone, J. Rohr, C.V. Catapano, Inhibition of Sp1-dependent transcription and antitumor activity of the new aureolic acid analogues mithramycin SDK and SK in human ovarian cancer xenografts, Gynecol. Oncol., 118 (2010) 182-188.
[19] M. Bataller, C. Méndez, J.A. Salas, J. Portugal, Mithramycin SK modulates polyploidy and cell death in colon carcinoma cells, Mol. Cancer Ther., 7 (2008) 2988-2997.
[20] C. Vizcaíno, S. Mansilla, L.E. Núñez, C. Méndez, J.A. Salas, F. Morís, J. Portugal, Novel mithramycins abrogate the involvement of protein factors in the transcription of cell cycle control genes, Biochem. Pharmacol., 84 (2012) 1133-1142.
[21] S. Safe, M. Abdelrahim, Sp transcription factor family and its role in cancer, Eur. J. Cancer, 41 (2005) 2438-2448.
[22] I. Wierstra, Sp1: Emerging roles—Beyond constitutive activation of TATA-less housekeeping genes, Biochem. Biophys. Res. Commun., 372 (2008) 1-13.

[23] M. Zhang, A. Mathur, Y. Zhang, S. Xi, S. Atay, J.A. Hong, N. Datrice, T. Upham, C.D. Kemp, R.T. Ripley, G. Wiegand, I. Avital, P. Fetsch, H. Mani, D. Zlott, R. Robey, S.E. Bates, X. Li, M. Rao, D.S. Schrump, Mithramycin represses basal and cigarette smoke-Induced expression of ABCG2 and inhibits stem cell signaling in lung and esophageal cancer cells, Cancer Res., 72 (2012) 4178-4192.
[24] S. Su, C.J. Omiecinski, Sp1 and Sp3 transcription factors regulate the basal expression of human microsomal epoxide hydrolase (EPHX1) through interaction with the E1b far upstream promoter, Gene 536 (2014) 135-144
[25] G. Suske, The Sp-family of transcription factors, Gene, 238 (1999) 291-300.
[26] A. López-Soto, A. Quiñones-Lombrana, R. López-Arbesu, C. López-Larrea, S. González, Transcriptional regulation of ULBP1, a human ligand of the NKG2D receptor, J. Biol. Chem., 281 (2006) 30419-30430.
[27] A. López-Soto, A.R. Folgueras, E. Seto, S. González, HDAC3 represses the expression of NKG2D ligands ULBPs in epithelial tumour cells: potential implications for the immunosurveillance of cancer, Oncogene, 28 (2009) 2370-2382.
[28] R.W. McGilvray, R.A. Eagle, P. Rolland, I. Jafferji, J. Trowsdale, L.G. Durrant, ULBP2 and RAET1E NKG2D ligands are independent predictors of poor prognosis in ovarian cancer patients, Int. J. Cancer 127 (2010) 1412-1420
[29] A.D. Malcolm, J.R. Moffatt, Differential reactivities at restriction enzyme sites, Biochim. Biophys. Acta, 655 (1981) 128-135.
[30] P.M. Yang, P.J. Lin, C.C. Chen, CD1d induction in solid tumor cells by histone deacetylase inhibitors through inhibition of HDAC1/2 and activation of Sp1, Epigenetics, 7 (2012) 390-399.
[31] M. Bataller, C. Méndez, J.A. Salas, J. Portugal, Cellular response and activation of apoptosis by mithramycin SK in p21^{WAF1}-deficient HCT116 human colon carcinoma cells, Cancer Lett., 292 (2010) 80-90.
[32] L.L. Remsing, H.R. Bahadori, G.M. Carbone, E.M. McGuffie, C.V. Catapano, J. Rohr, Inhibition of *c-src* transcription by mithramycin: structure-activity relationships of biosynthetically produced mithramycin analogues using the *c-src* promoter as target, Biochemistry, 42 (2003) 8313-8324.
[33] P.D. Grivas, H. Kiaris, A.G. Papavassiliou, Tackling transcription factors: challenges in antitumor therapy, Trends Mol. Med., 17 (2011) 537-538.
[34] V.A. Bloomfield, D.M. Crothers, I.J. Tinoco, Physical Chemistry of Nucleic Acids, Harper & Row, New York, 1974, p. 436.

[35] S. Mansilla, J. Portugal, Sp1 transcription factor as a target for anthracyclines: Effects on gene transcription, Biochimie, 90 (2008) 976-987.
[36] Y.A. Boumber, Y. Kondo, X. Chen, L. Shen, Y. Guo, C. Tellez, M.R. Estecio, S. Ahmed, J.P. Issa, An Sp1/Sp3 binding polymorphism confers methylation protection, PLoS Genet., 4 (2008) e1000162
[37] S.N. Westin, T.J. Herzog, R.L. Coleman, Investigational agents in development for the treatment of ovarian cancer, Invest. New Drugs 31 (2013) 213-229

LEGENDS TO FIGURES

Fig. 1. Chemical formulae of mithramycin A (MTA), mithramycin SK (MSK) and demycarosyl-3D-β-D-digitoxosyl-mithramycin SK (DIG-MSK). MTA differs from the other two analogues in the side chain linked to C-3. MSK and the structurally related DIG-MSK differ in sugar E in the trissacharide moiety.

Fig. 2. DIG-MSK binds to DNA. Fluorescence spectra of the complexes formed between Mg^{2+}-coordinated DIG-MSK dimers and DNA in 50 mM NaCl, 20 mM Hepes (pH 7.5) buffer containing 1.5 mM $MgCl_2$ at 25 ºC (A) and 37 ºC (B). The different complexes correspond to the titration of 22 μM compound (line 1) with 45, 70, 95 and 120 μM calf thymus DNA (lines 2, 3, 4 and 5, respectively). Adding higher DNA concentrations did not result in appreciable changes in fluorescence emission.

Fig. 3. Inhibition of restriction enzyme cleavage by mithramycins. (A) Representative agarose gels depicting the time course of cleavage of linearized pBR322 by *Bsp68I* or *Eco52I* restriction enzymes in the absence (control) or the presence of MTA, MSK or DIG-MSK. In the experiments depicted in the figure the drug/DNA (bp) molar ratio was 0.2, which corresponds to a stoichiometry of 5 mol of DNA (bp) per mol of mithramycin analogue. (B) Histograms represent the change in the rate of restriction cleavage by the presence of each mithramycin analogue (k) and in their absence (ko). Lower k/ko values (mean ± SD from three independent experiments, as those shown in panel A, indicate a higher degree of inhibition (**$p < 0.01$, *$p < 0.05$).

Fig. 4. Cellular and nuclear accumulation of MTA, MSK and DIG-MSK by A2780, OVCAR3 and IGROV1 human ovarian carcinoma cells. About $1x10^4$ viable cells were examined. Results represent the mean fluorescence intensity (a.u.) of the total cell population ± SEM for 4-6 independent experiments; *$p < 0.05$, comparing drug accumulation between 2-h and 4-h treatments.

Fig. 5. Effects of MTA and DIG-MSK on transcription driven by the Sp1 transcription factor in A2780, OVCAR3 and IGROV1 cells. (A) Relative changes in the luciferase activity of a transfected Sp1-reporter vector in the presence of 200 nM MTA or DIG-MSK, compared to control, untreated, cells (mean ± SD from six independent experiments; **$p < 0.01$). (B)

Luciferase activity in cells treated with 400 nM trichostatin A (TSA), followed by treatment with 200 nM MTA or DIG-MSK. TSA produced an enhancement of Sp1-transactivating activity, which was measured relative to control experiments in panel A (mean ± SD from six independent experiments; **p < 0.01, compared to TSA-treated cells). (C) Effects of 200 nM MTA or DIG-MSK on the expression of a transfected Sp1-luciferase reporter vector after co-transfection of the different cell lines with pN3-Sp1FL expression vector (mean ± SD from three independent experiments; **p < 0.01). (D) qRT-PCR analysis of the expression of the endogenous *Sp1* gene in the presence of 200 nM MTA or DIG-MSK, compared to untreated cells (mean ± SD from six independent experiments; **p < 0.01).

Fig. 6. Effects of MTA and DIG-MSK on transcription driven by the Sp3 transcription factor in A2780, OVCAR3 and IGROV1 cells. (A) Effects of MTA and DIG-MSK on luciferase reporter activity driven by the ULBP1 promoter (mean ± SD from six independent experiments; *p < 0.05, **p < 0.01). (B) Effects of 200 nM MTA or DIG-MSK on the expression of a transfected Sp1-luciferase reporter vector (which is also responsive to Sp3) after co-transfection of A2780, OVCAR3 and IGROV1 cells with pN3-Sp3FL expression vector (mean ± SD from three independent experiments; *p < 0.05, **p < 0.01). (C) Relative changes in the expression of *Sp3* gene in the presence of 200 nM MTA or DIG-MSK determined by qRT-PCR (mean ± SD from six independent experiments; **p < 0.01). (D) Relative changes in *ULBP1* expression in the presence of 200 nM MTA or DIG-MSK (mean ± SD from six independent experiments; *p < 0.05, **p < 0.01).

Fig. 7. Expression of a set of endogenous Sp-responsive genes in A2780, IGROV1 and OVCAR3 cells. Cells were treated with either 100 nM MTA, MSK or DIG-MSK for 24 h. Individual transcripts were quantified by qRT-PCR, normalized by the expression of the housekeeping *GAPDH* gene, and compared to untreated cells. (A) Relative gene expression in A2780 cells. (B) Relative gene expression in IGROV1 cells. (C) Relative gene expression in OVCAR3 cells. Data are mean ± SD from three to six independent experiments (*p < 0.05, **p < 0.01)

Table 1
Primers used for qRT-PCR analysis of the expression of some endogenous genes in human ovarian carcinoma cell lines. The housekeeping gene *GAPDH* was used for data normalization.

GENE	Primers	
Sp1	forward:	5'-AGAATTGAGTCACCCAATGAGAACA-3'
	reverse:	5'-GTTGTGTGGCTGTGAGGTCAAG-3'
Sp3	forward:	5'-CCAGGATGTGGTAAAGTCTA-3'
	reverse:	5'-CTCCATTGTCTCATTTCCAG-3'
CCNB1	forward:	5'-CAGGATAATTGTGTGCCCAAGA-3'
	reverse:	5'-TGGCAGTGACACCAACCAGT-3'
VEGF-C	forward:	5'-CTACAGATGTGGGGGTTGCT-3'
	reverse:	5'-GCTGCCTGACACTGTGGTAA-3'
E2F1	forward:	5'-AAGCGGCGCATCTATGACAT-3'
	reverse:	5'-AATGAGCTGGATGCCCTCAA-3'
ULBP1	forward:	5'-ATCAGCGCCTCCTGTCCAC-3'
	reverse:	5'-AAAGACAGTGTGTGTCGACCCAT-3'
GAPDH	forward:	5'-CTCTGCCCCCTCTGCTGAT-3'
	reverse:	5'-CTTCTCATGGTTCACACCCATG-3'

Table 2
Effects of mithramycin A (MTA), mithramycin SK (MSK) and demycarosyl-3D-β-D-digitoxosyl-mithramycin SK (DIG-MSK) on the melting temperature of calf thymus DNA (Tm)[a]

	r[b]	Tm (ºC)[c]	ΔTm (ºC)
DNA	—	86.9 ± 0.3	—
MTA	0.25	90.2 ± 0.4	3.3
MSK	0.25	89.0 ± 0.5	2.1
DIG-MSK	0.25	87.6 ± 0.3	0.7

[a] DNA melting curves were measured in 50 mM NaCl, 1 mM $MgCl_2$, 20 mM Hepes (pH 7.5)
[b] **r** = drug/DNA (bp) molar ratios; **r** = 0.25 corresponds to a binding stoichiometry of 4 mol of bp per mol of drug, enough to saturate the potential binding sites [16].
[c] Mean ± SD values from three independent experiments.

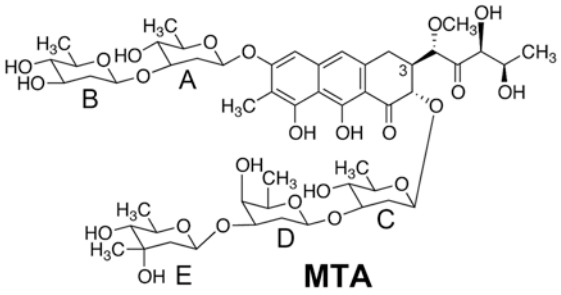

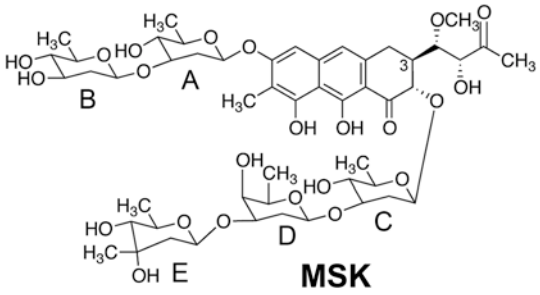

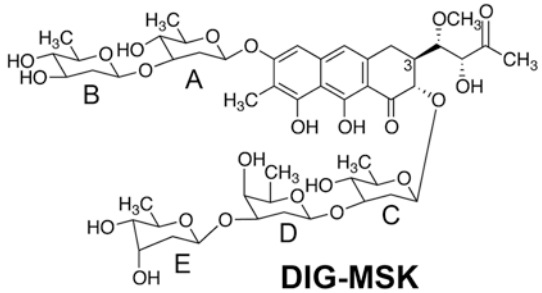

Figure1

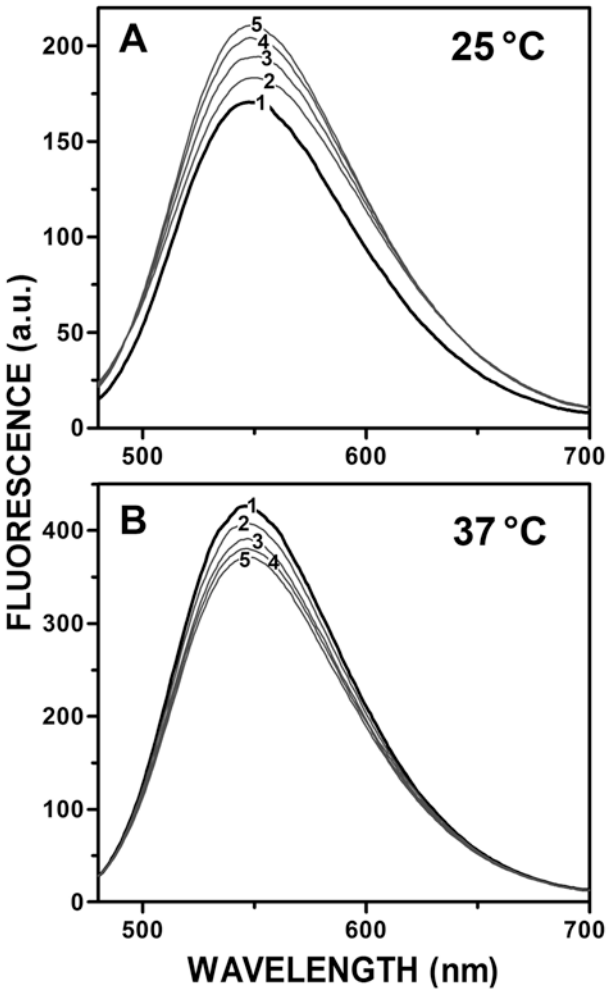
A
25 °C
5
4
3
2
1
200
150
100
50
0
500
600
700
B
37 °C
1
2
3
5
4
400
300
200
100
0
500
600
700
FLUORESCENCE (a.u.)
WAVELENGTH (nm)

Figure 2

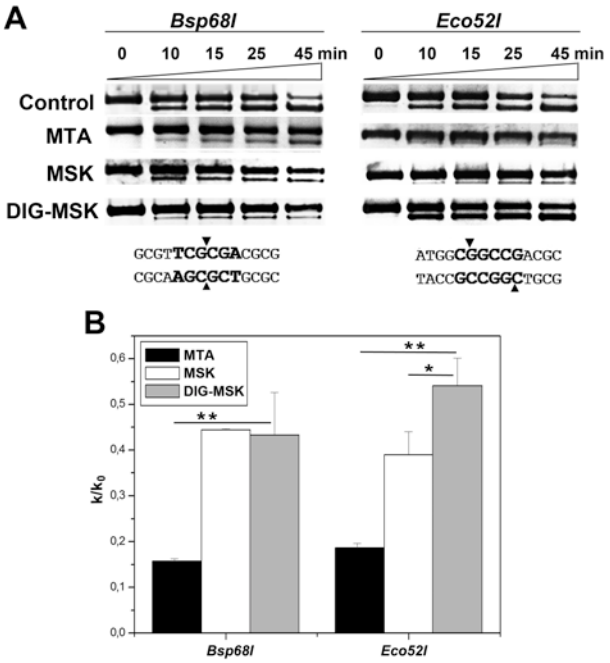
A
Bsp68I
Eco52I
0 10 15 25 45 min
0 10 15 25 45 min
Control
MTA
MSK
DIG-MSK
GCGTTCGCGACGCG
CGCAAGCGCTGCGC
ATGGCGGCCGACGC
TACCGCCGGCTGCG
B
MTA
MSK
DIG-MSK
k/k0
0,0
0,1
0,2
0,3
0,4
0,5
0,6
**
**
*
Bsp68I
Eco52I

Figure 3

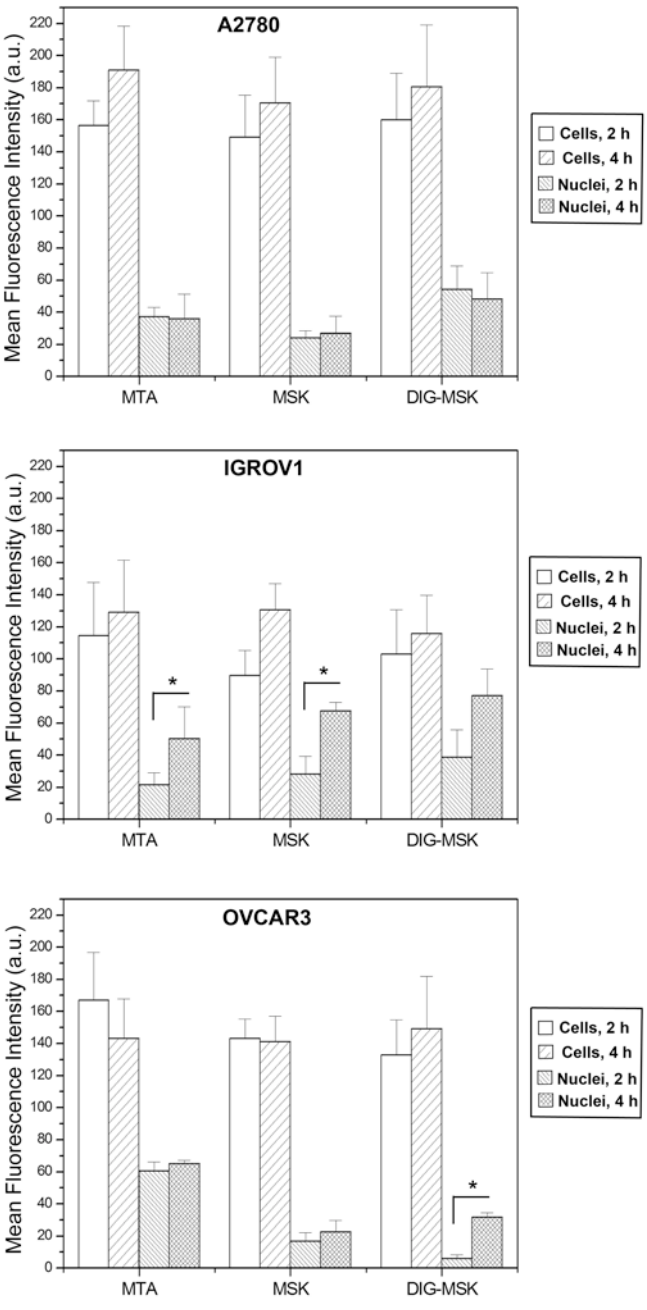
A2780
IGROV1
OVCAR3
Mean Fluorescence Intensity (a.u.)
MTA
MSK
DIG-MSK
Cells, 2 h
Cells, 4 h
Nuclei, 2 h
Nuclei, 4 h
*

Figure 4

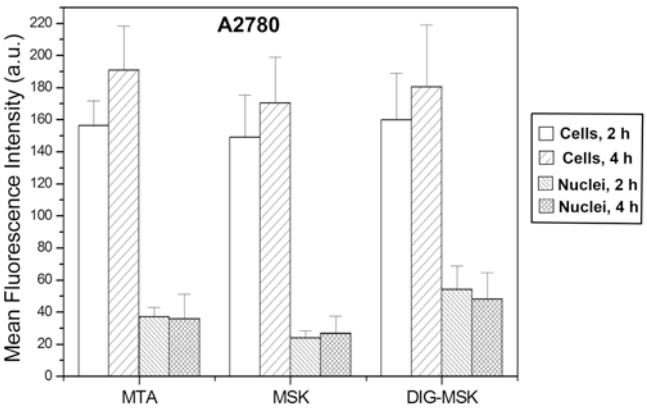
A2780
Mean Fluorescence Intensity (a.u.)
0
20
40
60
80
100
120
140
160
180
200
220
MTA
MSK
DIG-MSK
Cells, 2 h
Cells, 4 h
Nuclei, 2 h
Nuclei, 4 h

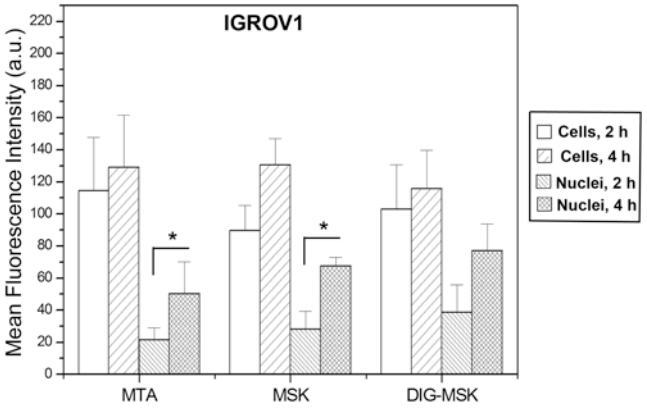
IGROV1
Mean Fluorescence Intensity (a.u.)
0
20
40
60
80
100
120
140
160
180
200
220
*
*
MTA
MSK
DIG-MSK
Cells, 2 h
Cells, 4 h
Nuclei, 2 h
Nuclei, 4 h

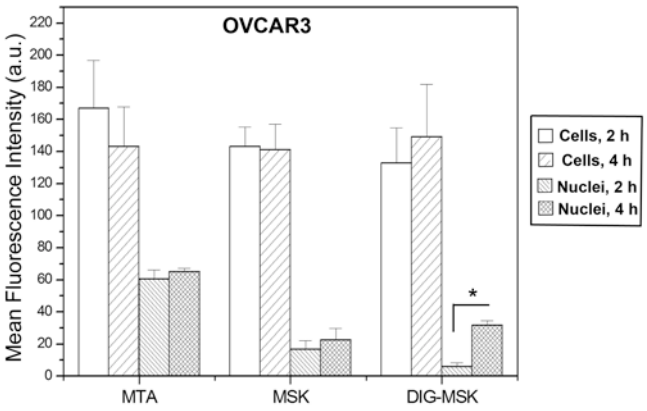
OVCAR3
Mean Fluorescence Intensity (a.u.)
0
20
40
60
80
100
120
140
160
180
200
220
*
MTA
MSK
DIG-MSK
Cells, 2 h
Cells, 4 h
Nuclei, 2 h
Nuclei, 4 h

Figure 4

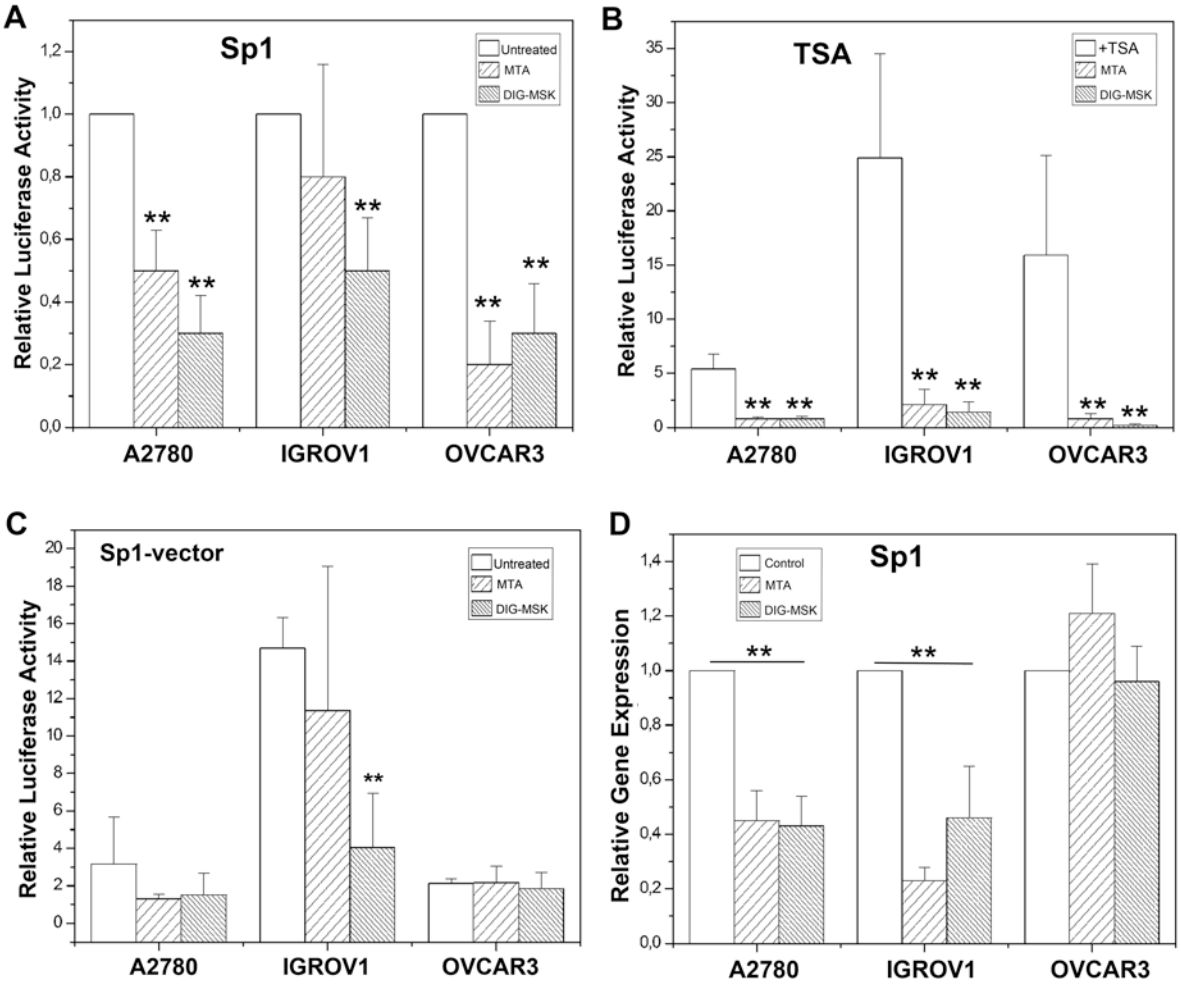
A
Sp1
Untreated
MTA
DIG-MSK
Relative Luciferase Activity
1,2
1,0
0,8
0,6
0,4
0,2
0,0
**
A2780
IGROV1
OVCAR3
B
TSA
+TSA
MTA
DIG-MSK
Relative Luciferase Activity
35
30
25
20
15
10
5
0
**
A2780
IGROV1
OVCAR3
C
Sp1-vector
Untreated
MTA
DIG-MSK
Relative Luciferase Activity
20
18
16
14
12
10
8
6
4
2
0
**
A2780
IGROV1
OVCAR3
D
Sp1
Control
MTA
DIG-MSK
Relative Gene Expression
1,4
1,2
1,0
0,8
0,6
0,4
0,2
0,0
**
**
A2780
IGROV1
OVCAR3

Figure 5

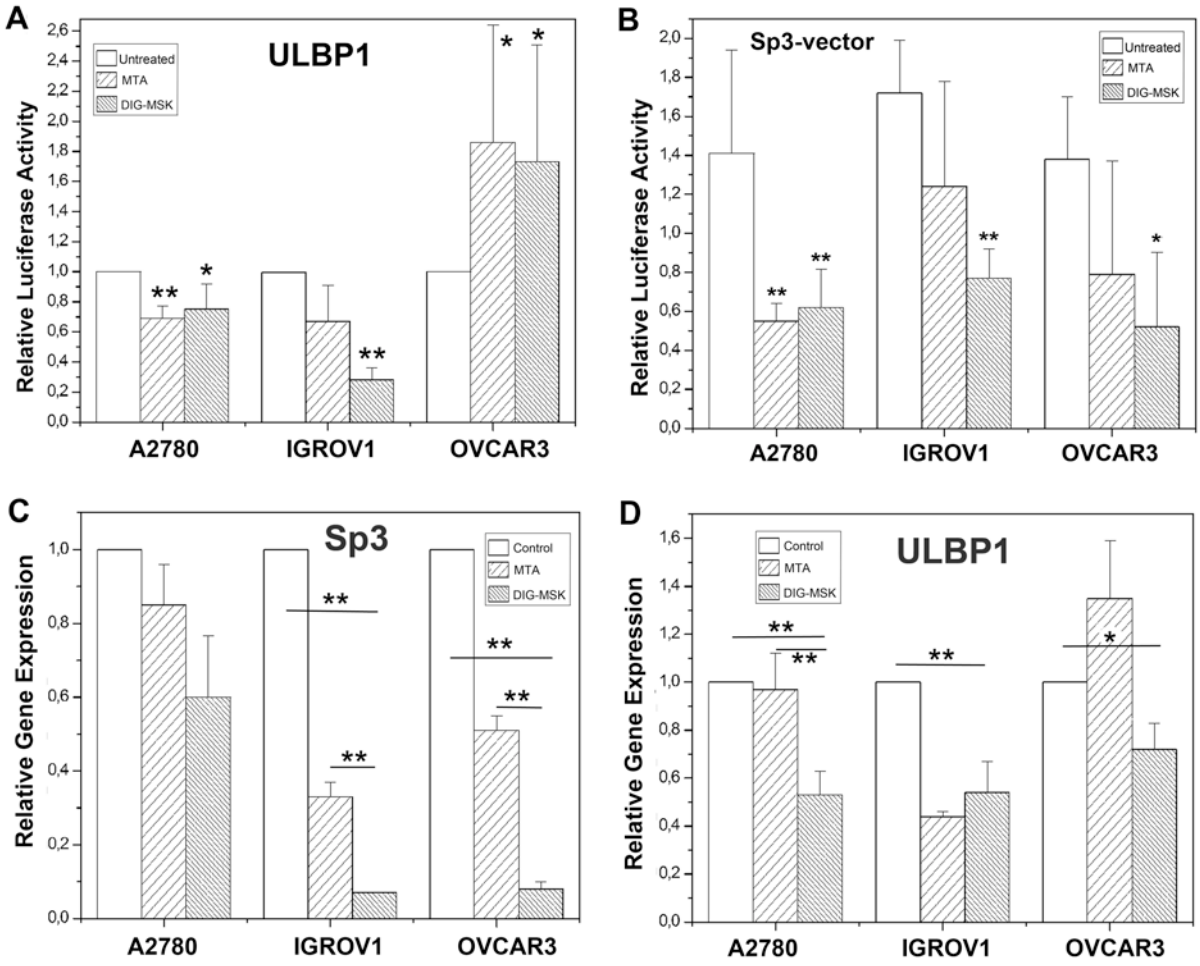
A
ULBP1
Untreated
MTA
DIG-MSK
Relative Luciferase Activity
A2780
IGROV1
OVCAR3
B
Sp3-vector
C
Sp3
Control
Relative Gene Expression
D
ULBP1

Figure 6

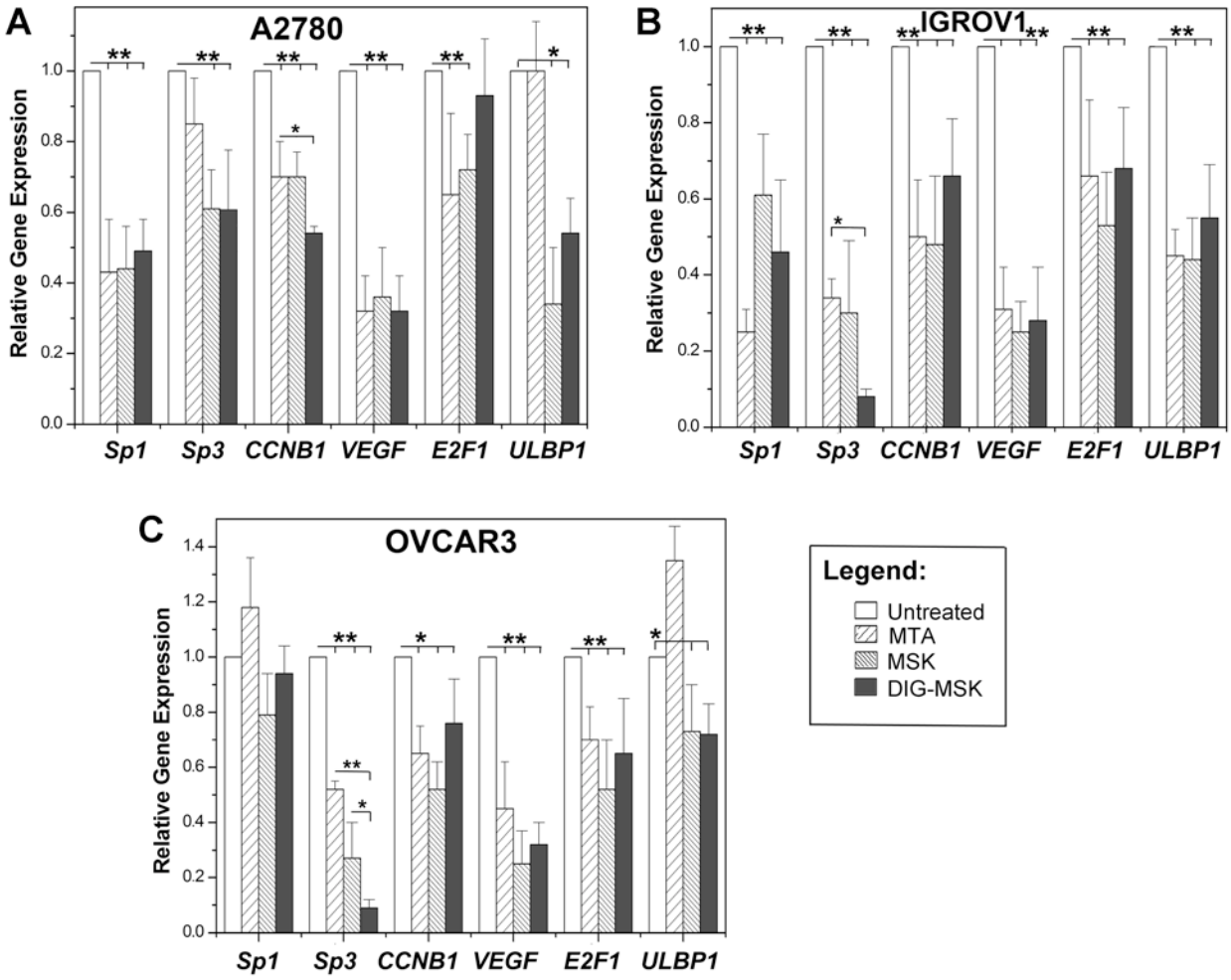
A
A2780
B
IGROV1
C
OVCAR3
Relative Gene Expression
Sp1
Sp3
CCNB1
VEGF
E2F1
ULBP1
Legend:
Untreated
MTA
MSK
DIG-MSK

Figure 7